

ETHYLENE FROM RENEWABLE ETHANOL: PROCESS OPTIMIZATION AND ECONOMIC FEASIBILITY ASSESSMENT

Martina Frosi^a, Antonio Tripodi^a, Francesco Conte^a, Gianguido Ramis^b, Nader Mahinpey^c and
Ilenia Rossetti^{a*}

^a Chemical Plants and Industrial Chemistry Group, Dipartimento di Chimica, Università degli Studi
di Milano, INSTM Milano Università-Unit, Via Golgi 19, 20133 Milano (MI) – Italy

^b Dip. Ing. Chimica, Civile ed Ambientale, Università degli Studi di Genova and INSTM Unit
Genova, Via all'Opera Pia 15A, 16145 Genoa, Italy

^c Dept. of Chemical and Petroleum Engineering, University of Calgary 2500 University Drive NW,
Calgary, AB T2N 1N4 Canada

ABSTRACT

At present, ethylene is the most widely produced organic compound in the chemical industry. The main commercial way to obtain ethylene is by steam cracking of a wide range of hydrocarbon feedstocks, but biomass-derived ethanol can be catalytically dehydrated as a sustainable alternative route in order to exploit new renewable sources. The aim of this work is to design an optimal

* Corresponding author: fax +390250314300; email ilenia.rossetti@unimi.it

bioethanol-to-bioethylene plant, with a capacity of 445,652 ton/year, and to assess its economic feasibility. This design features an improved production capacity and intensified energy management. The main novelty of this study is the use of diluted bioethanol solutions, bypassing the energy intensive and expensive dehydration step. Moreover, while the first industrial bioethanol-to-bioethylene process uses NaOH to purify the outcoming flow from CO₂, this plant uses diluted Methyldiethanolamine (MDEA), regenerated in situ. With this plant, the double of the capacity of the Braskem's plant, now the largest one, can be reached in an environmentally more sustainable manner. A pinch analysis was performed, in order to minimize the energy consumption of the process by optimizing the heat recovery systems. The economic analysis of the process consists of the evaluation of the total cost of the plant (TOC) including the sum of the CAPital EXpenditures (CAPEX) and the OPerating ones (OPEX), together with some sensitive profitability indexes (net yearly profit, net present value, net rate of return and cash flow analysis). The designed process presents an economically competitive solution compared to the current bioethylene production units. Assuming a premium price of between 0.293 \$/kg for diluted bioethanol, the proposed plant is competitive with the lowest production cost for bioethylene (Brazil and India), while a sensitivity analysis on diluted bioethanol price evidenced that this option remains competitive still in Europe with a bioethanol cost 0.65 \$/kg.

Keywords: Bioethylene; Bioethanol; Biorefinery; Economic assessment; Process Intensification; Energy Integration.

LIST OF SYMBOLS

A_A	Allowances
A_{BD}	Depreciation
A_{CI}	Annual Cash Income
A_{DME}	Total Direct Operating Cost
A_{EDR}	Aspen Exchanger Design and Rating
A_{GE}	General Expenses
A_I	Annual Capital Investment
A_{IME}	Total Indirect Operating Cost
A_{IT}	Income Taxes
A_{ME}	Manufacturing Expenses
A_{NCI}	Annual Net Cash Income
A_{NNP}	Net Annual Profit after Taxes
A_{NP}	Net Annual Profit
AP	Aspen Plus
$APEA$	Aspen Process Economic Analyzer
As	Revenue from Sales
A_{TE}	Total Operating Expenses
$CAPEX$	Capital Expenses
$CEPCI$	Chemical Engineering Plant Cost Index
C_{FC}	Fixed Capital
C_{TC}	Total Capital Expenses
C_{WC}	Working Capital
$DBEP$	Discounted break-even point
DCF	Discounted Cash Flow Analysis
df	Discount Factor
F	Lang Factor
$ISBL$	Inside Battery Limits
$LHHW$	Langmuir-Hinshelwood-Hougen-Watson model
$MDEA$	Methyldiethanolamine
n'	Operating lifetime plus one-half the time proceeding the start-up in years
NPV	Net Present Value economic analysis
NRR	Net Rate of Return
$NRTL$	Non random two liquids, thermodynamic model
$OPEX$	Operating Expenses
$OSBL$	Outside Battery Limits
PBP	Payback-period
PSA	Pressure swing Adsorption
RK	Redlich Kwong, thermodynamic model
S	Salvage Value

1 INTRODUCTION

The first commercial plant to produce ethylene from ethanol was built and operated at Elektrochemische Werke G.m.b.H at Bitterfeld, Germany in 1913. It was a small-scale plant, using alumina as catalyst in isothermal conditions, to produce ethylene for the preparation of pure ethane as refrigerant. The alumina catalyst, despite its many disadvantages, reached a very high ethylene purity required for polyethylene polymerization. During the 1950s, ethylene was made from oil-based steam cracking plants. In 1980s, ethanol-based ethylene plants started to be built in India, Pakistan, Australia, Peru, and Brazil with capacities between 3,000 and 30,000 tons/year and the biggest one was operated by Salgema (Braskem) in Brazil with a capacity of 100,000 tons/year, to produce ethylene dichloride and then polyvinyl chloride. Later, following the drop of oil price, almost all these plants were shut down, until 2007, when Braskem started the operation of a new pilot plant for bio-based ethylene to produce polyethylene [1].

At present, ethylene is the most widely produced organic compound in the chemical industry. Its world annual production is 134 million tons. It is used to produce polyethylene (PE, 80 million tons/year), ethylene oxide (EO, 21 million tons/year), ethylene glycol (EG, 6.7 million tons/year), vinyl chloride monomer (VCM) for polyvinyl chloride (PVC, 38.5 million tons/year) and styrene (26.4 million tons/year). Besides these main products, linear alpha olefins (LAO), detergent alcohols and plasticiser alcohols, vinyl acetate monomer (VAM), and various intermediates such as ethyl acetate and ethyl acrylate are also produced. Thus, ethylene production is one of the indicators of the petrochemical development level of a country [2].

The main production process for ethylene is steam cracking of hydrocarbon feedstocks. In Europe and Asia, ethylene is obtained mainly from naphtha, gasoil and condensates. In Contrast, ethane and propane are the main feeds in the US, Canada and the Middle East. As mentioned, the catalytic dehydration of biomass-derived ethanol is an alternative, to exploit cheap and renewable sources in an integrated biorefinery concept. The bio-polymer market is growing fast: the present supply is lower than 1%, while the demand for renewable polyethylene approaches 10% of the market [3–6].

Ethanol dehydration reaction is endothermic and is catalysed by acids. Most of the ethanol-to-ethylene dehydration processes use alumina catalysts, loaded in multitube or adiabatic fixed-bed reactors [7]. However, alumina deactivates by carbon deposition and, as the common solution, steam is added to prevent extensive deactivation. The deactivation may limit the reactivity thermodynamically; and, kinetically, it may influence the reaction due to the competitive adsorption between ethanol and water.

Top industrial ethanol-to-ethylene plants are those of Braskem (Brazil, 200,000 ton/year), Dow Chemical Company (Brazil, under construction, 190,000 ton/year) and Solvay Indupa (Brazil, 60,000 ton/year) [8]. Their capacities are much lower than those of steam cracking plants (1,650,000-2,935,000 ton/year). Therefore, they adapt well to biomass exploitation in small delocalised biorefineries, but they cannot take advantage of large scale [8–13]. As a result, careful process optimisation, the use of inexpensive feedstocks and the search for economic feasibility boundaries are compulsory to ensure the success of this ethylene production routes.

Our research group demonstrated the application of diluted bioethanol solutions, while taking into account the possible impurities present in such less purified feed [14–18]. The aim of this work is the design, optimisation and economic feasibility assessment of a bioethanol-to-bioethylene plant, starting from a 40 vol% solution of bioethanol as an inexpensive feedstock. Indeed, its production only requires the concentration of the fermentation broth through a flash drum. Optimisation of the plant layout and of the energy management were additional goals. Finally, the capital and operating expenditures, as well as the main profitability indexes have been calculated to establish the feasibility of this solution, that would be a step towards sustainability of ethylene production with respect to fossil routes.

2 MODELS AND METHODS

The simulation of the plant was performed using Aspen Plus V10 (Aspentech Inc., AP V10). Aspen Exchanger Design and Rating (AEDR V10) was used to size the heat exchangers. The cost of reactors,

flash drum separators, towers, pumps, compressors and mixers was evaluated using Aspen Process Economic Analyser (APEA V10). The costs of the PSA were evaluated according to [19]. To evaluate the costs of the heat exchangers Aspen EDR was used.

2.1 Reaction mechanism

Ethanol dehydration is endothermic and occurring at relatively high temperature (350-450°C) [20]. Various mechanisms were proposed, depending on the catalyst and process conditions. Over alumina, ethylene is produced from ethanol via either monomolecular (1) and bimolecular (2,3) dehydration [7].



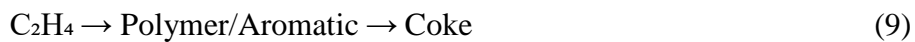
At 150-300 °C diethyl ether is commonly the main product, while at higher temperature (400-500°C) ethylene selectivity decreases, forming higher hydrocarbons and aromatics. Thus, the possible major by-products are diethyl-ether (2), acetaldehyde (4) and butene (5).



Other possible by-products are methane, ethane, propylene, CO₂, CO, H₂, etc.



Recently, the unconventional use of a diluted ethanol solution (*ca.* 40 vol%, 50 wt%) for ethylene production proved successful, thus limiting very much the ethanol purification costs (only flash purification of the fermentation broth with respect to azeotropic distillation) and preventing catalyst coking (9) [16].



2.2 Reaction kinetics

The kinetics of the reactions was previously studied [18]. The reactions 1 - 5 were modelled with the Langmuir Hinshelwood Hougen Watson model (LHHW), whereas the reactions 6 and 7 with a power rate law (POWERLAW) model. The latter is also known as the Ostwald–de Waele power law. This mathematical relationship is useful because of its simplicity, but only approximately describes the behaviour of a real non-Newtonian fluid [21]. For the LHHW class, the rate can be written as:

$$r = \frac{[\text{Kinetic Factor}, k][\text{Driving Force}]}{[\text{Adsorption}]}$$

whereas for the POWERLAW class:

$$r = [\text{Kinetic Factor}][\text{Driving Force}]$$

The kinetic factor is always calculated by the Arrhenius law:

where T_0 is specified:

$$k = k_0 \left(\frac{T}{T_0} \right)^n e^{\frac{-\Delta E_a}{R} \left(\frac{1}{T} - \frac{1}{T_0} \right)}$$

where T_0 is not specified:

$$k = k_0 e^{\frac{-\Delta E_a}{RT}}$$

where k_0 is the pre-exponential factor, whose units depends on the reaction order, ΔE_a is the activation energy of the reaction, T is temperature and R is the universal gas constant.

The power law model is represented by the following general formula:

$$r_j = k_j \prod_i y_i^{v_{ij}}$$

Where r_j is the dimensionless reaction rate, j is the number of the reaction, k_j is the specific reaction rate, y_i is the dimensionless molar concentration of each component, v_{ij} is the stoichiometric coefficient of the i -th component in the j -th reaction and v_j is the overall reaction order.

The LHHW model includes an adsorption term:

$$[Adsorption\ expression] = [Term1 + Term2 + \dots]^{Ads\ exp}$$

Where

$$Term_i = K_i * [C_2H_5OH]^m * [H_2O]^m$$

and

$$\ln K_i = A + \frac{B}{T} + C \ln T + DT$$

The adsorption parameters needed for each reaction are the adsorption expression exponent, the concentration exponents n_i , and the adsorption constant K_i . The parameters used to build the kinetic model in Aspen Plus are reported in Tables 1 and 2.

Table 0: Kinetic parameters for the adopted models [18].

Reaction	Rate unit (Rate basis: Cat (wt.))	k_i	n_i	E_a (kJ/mol)	T_0 (°C)
(1)	mol/g s	6.84e-06	0	66.5	300
(2)	mol/g s	0.249	0	63.9	300
(3)	mol/g s	0.000557	0	107	300

(4)	mol/g s	3.07e-05	0	60	300
(5)	kmol/kg s	0.001	0	114	300
(6)	mol/g s	1.13e-07	0	122.9	625
(7)	mol/g s	3.06e-07	0	195.5	625

Table 2 Adsorption parameters for the selected models [18].

Reaction	Term _i	A	B, C, D	K _i	m _i C ₂ H ₅ OH	m _i H ₂ O	Ads. Exp.	Ads expression
(1)	1	0	0	1	0	0	1	{K1+K2[C ₂ H ₅ OH] +K3[H ₂ O]}
	2	3.85	0	47	1	0		
	3	2.86	0	17	0	1		
(2)	1	0	0	1	0	0	2	{K1+K2[C ₂ H ₅ OH] +K3[H ₂ O]} ²
	2	3.85	0	47	1	0		
	3	2.86	0	17	0	1		
(3)	1	0	0	1	0	0	1	{K1+K2[C ₂ H ₅ OH] +K3[H ₂ O]}
	2	3.5	0	33	1	0		
	3	2.86	0	17	0	1		
(4)	1	0	0	1	0	0	1	{K1+K2[C ₂ H ₅ OH] +K3[H ₂ O]}
	2	3.5	0	33	1	0		
	3	2.86	0	17	0	1		
(5)	1	0	0	1	0	0	2	{K1+K2[C ₂ H ₅ OH] +K3[H ₂ O]} ²
	2	3.85	0	47	1	0		
	3	2.86	0	17	0	1		

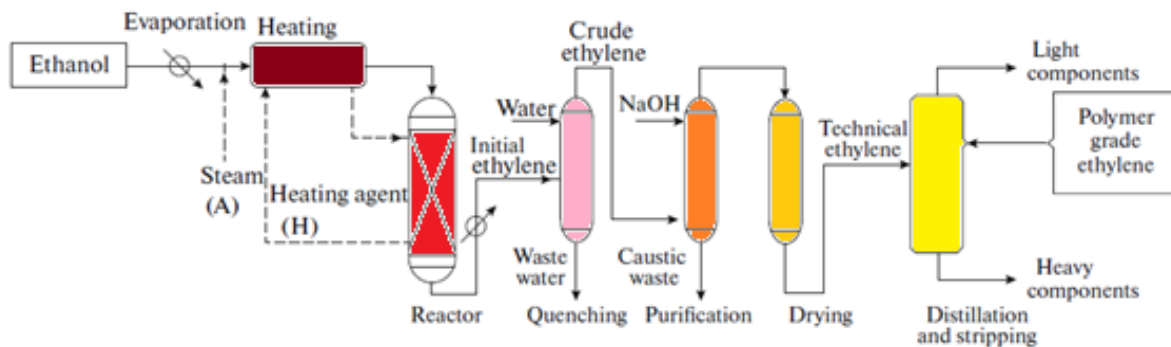
2.3 Thermodynamic model

From previous studies, the Non Random Two Liquids better computes the non ideality in liquid phase, coupled with the Redlich-Kwong equation of state for the gas phase (NRTL-RK). For steam and water, the model STEAM-TA has been used, while for the electrolytes, ELECNRTL-RK. For air and the cryogenic distillation the predictive Soave-Redlich-Kwong model (PSRK) was employed. The Henry constant for the mixture H₂, C₄H₈, C₂H₄, CO and CH₄ has been used for the separation units (flash, distillations, absorber and stripper).

3 PLANT LAYOUT

Ethanol dehydration is generally performed in gas phase with 95 vol% ethanol, at 200-500°C and with hourly space velocity 0.5 - 3 h⁻¹. High conversion and selectivity to ethylene are typically achieved. A simplified Process Flow Diagram (PFD) is represented in Figure 1 [1]. The feed is pre-heated before the reactor, then the product is first separated in an absorption column, followed by CO₂ removal with NaOH and drying. Finally, the dry mixture enters a cryogenic distillation column from the top of which polymer grade ethylene outflows.

Figure 1 Representation of a generic PFD of an ethanol-based ethylene plant [1].

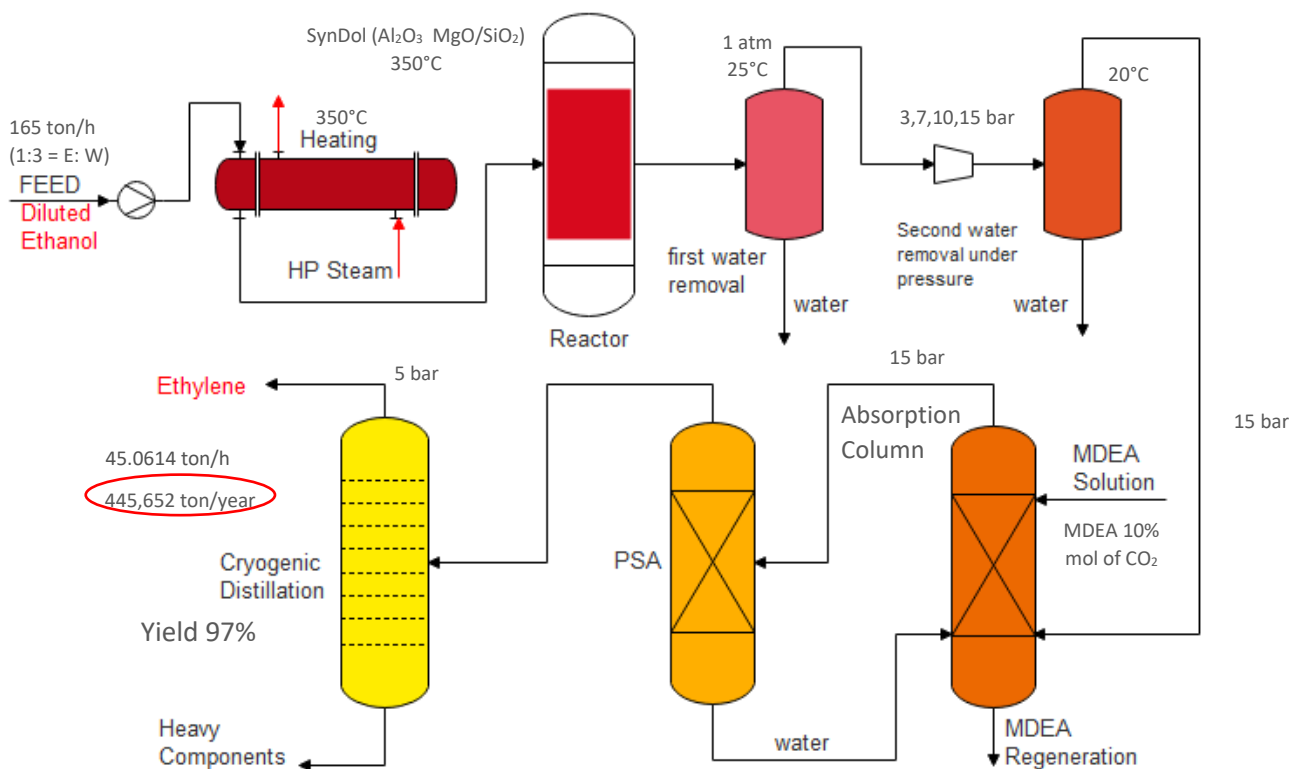


We propose here for the first time a new plant design, for a yearly production of *ca.* 400,000 ton/year (Figure 2). The feed consists of 165 ton/h of diluted ethanol (1 : 3 mol/mol = E : W) that are heated to 350°C and sent to a series of three fixed bed reactors. We have based this choice on the expertise of our research group with the exploitation of diluted bioethanol streams for this application and for the steam reforming to produce hydrogen and syngas [22]. The composition of a diluted bioethanol stream is exemplified elsewhere, where the content of higher alcohols that may lead to higher olefins by-products is considered [22].

Depending on the operating conditions, the reacting section allows to reach an ethanol conversion of *ca.* 90% per pass, overall 100% recycling the unconverted ethanol, while maintaining a minimum selectivity of 60%. A first coarse separation is performed in a flash drum at atmospheric pressure and ambient temperature. The mixture passes through a series of compressions and separations each one

at increasing pressure. CO₂ is removed by scrubbing with diluted MDEA. The latter is regenerated *in situ* and recycled, a greener and more sustainable approach with respect to the caustic wash used in traditional plants, in which salt formation occurs and needs disposal and fresh supply of caustic soda or potash. Our new approach also allows to recover CO₂ for storage or re-use. The last traces of water are removed in a two beds PSA, from which the dried chemical grade ethylene exits and feeds a cryogenic distillation column, from the top of which polymer grade ethylene is obtained. We report in the following some of the results obtained through the present simulation.

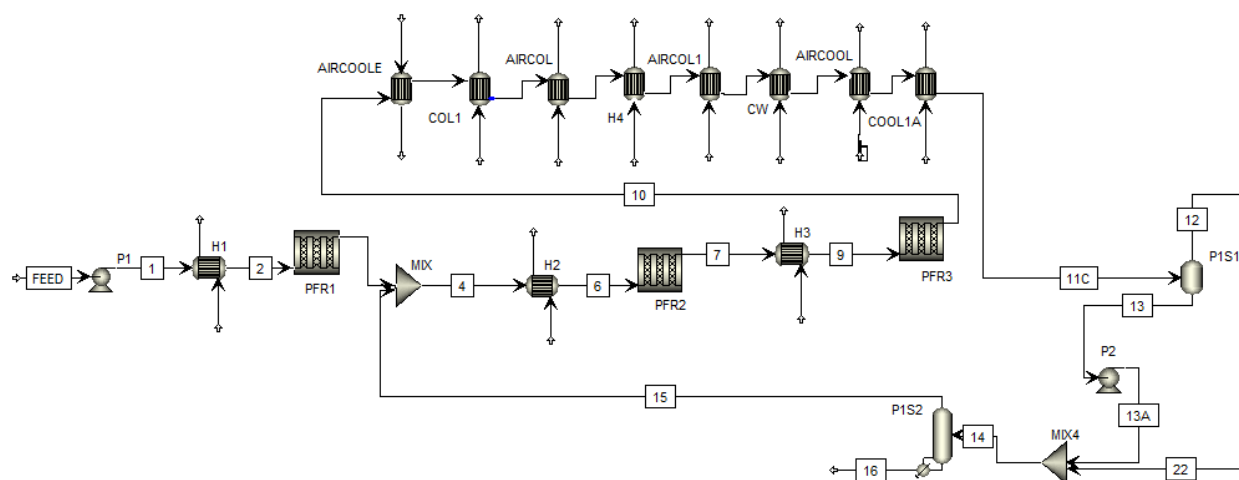
Figure 2 General scheme of the new ethanol-to-ethylene plant studied. For simplicity the recycle of ethanol is omitted, being detailed in the following Figure 3.



3.1 Reaction section

The detailed sketch of the reaction section is reported in Figure 3.

Figure 3 Reaction Section



The feed, 6,600 kmol/h of diluted (25 mol%) bio-ethanol at 25°C and 1 bar, is pumped at a pressure of 1.2 bar into the first adiabatic reactor stage (PFR1), after preheating at 350°C (H1) with HP steam at 390°C, 40 bar. The reaction mixture is mixed with the unreacted ethanol recycled through stream 15 and enters the second adiabatic reactor (PFR2) after preheating (H2). Again, being the reaction endothermic, the product of the second reactor is heated from 268°C to the target temperature (H3) and enters the third adiabatic reactor (PFR3). The streams exiting from the three reactors are detailed in Tables from S1 to S3 in the Supporting Information.

The pressure drop is computed using the Ergun equation with a scaling factor of 1 and roughness of 1 mm. We carried out a sensitivity analysis to optimize catalyst loading, resulting in 100 kg, 160 kg and 120 kg for the PFR1, PFR2 and PFR3, respectively. The product is cooled before entering the first flash separator (P1S1) working at 25°C, 1 bar, through a series of air coolers and cooling water heat exchangers (in and out temperatures 30 and 45°C, respectively), to diminish the amount of cooling water. The liquid from the bottom of the flash drum is pumped at 1.1 bar and sent, together with the recycle (stream 22), to the top of the stripping column (P1S2). This column has been specified with 13 trays, a Murphree efficiency of 70%, without condenser and with a distillate rate of

600 kmol/h. The stream compositions from P1S1 and P2S2 are reported in Tables from S4 to S7, while the heat flow in the heat exchangers and their areas are reported in Table S8.

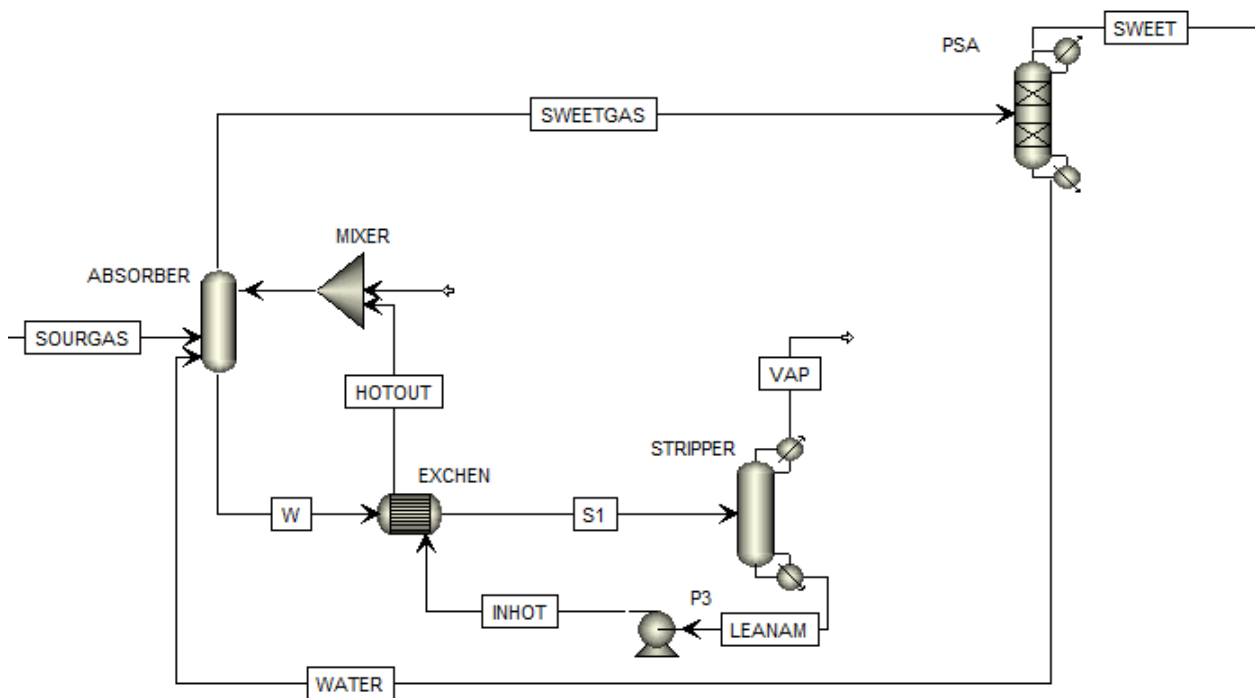
3.2 Separation section

The stream 12, exiting from the reaction section, passes through a series of compressors and separators at increasing pressure (Figure S1, Supporting Information). The first compressor works at 3 bar, consuming 1,981 kW and the compressed stream at 114°C is cooled first with an air cooler to 55°C and then with a refrigerant to 25°C, before feeding the first flash separator (SEP1). The vapour stream from SEP1 is compressed to 7 bar, consuming 1,432 kW, and from 87°C it is cooled again as above described to 25°C to reach SEP2. The third and the fourth steps operate at 10 and 15 bars consuming respectively 572 and 653 kW during the compression steps. From the top of SEP4, the SOURGAS stream exits and enters the absorption column. The bottom of each flash is stripped in P1S2 and is fed back to PFR2 to recycle the un-reacted ethanol. The process stream, SOURGAS, together with WATER, recycled from the bottom of the PSA, are sent to the bottom of the absorber (specified with 13 trays, 15 bar and a Murphree efficiency of 50%) where CO₂ is removed. Indeed, the discharge of water, which avoids the build-up and ensures the mass balance, occurs through the partial condenser of the MDEA regenerator. The PSA waste must be recycled somewhere upstream, because in our PSA strategy (*vide infra*) the beds are regenerated by a part of the dry ethylene, that cannot be wasted. The two obvious choices are to recycle damp ethylene to the first water condenser upstream the CO₂ capture, or right at the CO₂ capture inlet. The bottom of the absorber is the right point (when the second choice is made), because the PSA waste is actually a gaseous current.

To accomplish carbon dioxide separation we propose washing counter-current with aqueous MDEA (N-Methyldiethanolamine), with a stoichiometric factor of 1 mol of MDEA to trap 0.5 mol of CO₂ [23] (Figure 4). The spent amine is then regenerated in a stripping column at atmospheric pressure (10 trays, reflux ratio of 5, distillate to feed ratio of 0.09 and Murphree efficiency of 50%).

CO₂ is released from the top of the stripping column, whereas the regenerated MDEA is recycled from the bottom of the regenerator to the top of the absorber. Heat is recovered through EXCHEN, specified with a hot outlet-cold inlet temperature difference of 10°C. Streams composition are collected in Tables from S9 to S23 (Supporting Information).

Figure 4 CO₂ removal with aqueous MDEA and final drying with PSA



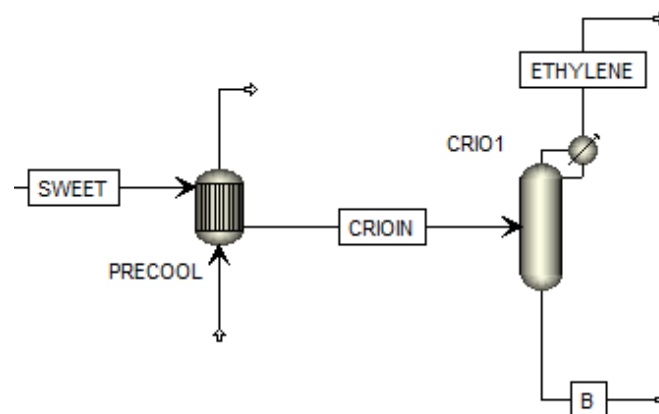
3.3 Purification Section

The SWEET stream, containing chemical grade ethylene from the PSA is precooled to -40°C before entering a cryogenic column from which polymer grade ethylene is obtained. Pre-cooling is achieved using ethane as utility that enters at -90°C to exit at -89°C. The duty is 1,122 kW, calculated without considering fouling, dispersions or efficiency. The cryogenic column (Figure 5) has been specified with 13 trays, distillate-to-feed ratio of 0.98 and a Murphree efficiency of 70%. The condenser removes 824 kW from the distillate. The compositions of the distillate and the bottom are reported in Tables S25 and S26 (Supporting Information). This last purification unit can cope also the case of

non nil formation of higher olefins in case higher alcohols may remain in the poorly refined diluted bioethanol.

Such composition of the purified stream accomplishes the purity requirements for polymer grade ethylene (>99.9 mol%), which are discussed in the relevant literature (see e.g. [24,25]).

Figure 5 Cryogenic Distillation



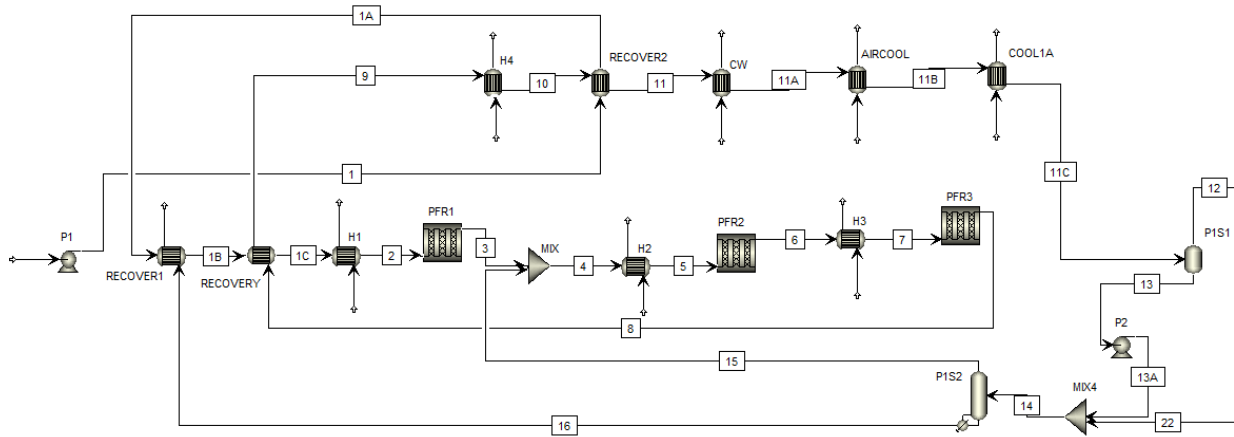
4 OPTIMIZATION OF THE ENERGY MANAGEMENT

Heat integration analysis aims at minimizing the energy consumption of a chemical process through optimization of the heat recovery systems, the energy supply methods and process operating conditions. A sequential strategy is applied: the process is optimized at first assuming all heating and cooling loads provided by utilities; then heat integration is performed after the optimal stream conditions (flow rates, temperatures, etc.) are identified through a retrofit approach. The flowsheet described in the previous paragraph is nominated as *non-integrated* and has been used to identify the possible energy savings, while the one with optimized heat exchange network is now called *retrofitted*.

The total heat provided by the external hot utility is 14,873 kW and the total heat withdrawn by the cold utility is 123,850 kW. The hot utility and the cold utility targets are respectively 104,940 kW and 80,117 kW.

From this analysis, the reaction section changes as shown in Figure 6 whereas the separation and purification sections remain unaltered. The streams compositions of the retrofitted reaction sections are the same reported in Tables S1-S3.

Figure 6 Reaction section - retrofitted process



5 SHORT-CUT EQUIPMENT DESIGN

Short-cut equipment design defines the capital cost with an accuracy of $\pm 25\%$, leaving the uncertainty in annual cost lower than 8% [19]. The entire plant has been designed in stainless steel. Conventional design procedures have been followed. The details on flash drums are reported in Tables 3 and 4.

Table 3 Inputs Flash Drums sizing

Name	ρ_l (kg/m ³)	ρ_v (kg/m ³)	V_v (m ³ /s)	u_t (m/s)	u_s (m/s)	V_l (m ³ /s)	V_l (m ³)	H_l (m)
P1S1	977.0	0.42	33.9	3.38	0.51	0.039	11.6	0.17
SEP1	889.47	3.46	3.77	1.12	0.17	0.001	0.361	0.016
SEP2	792.68	8.07	1.60	0.69	0.10	0.0001	0.0390	0.0025
SEP3	751.73	11.53	1.120	0.561	0.084	4.4E-05	1.3E-02	1.0E-03
SEP4	706.60	17.29	0.745	0.442	0.066	4.9E-05	1.5E-02	1.3E-03

Table 4 Output: Flash drums sizes

Name	D _v (m)	H (m)	H/D
P1S1	9.5	15	1.56
SEP1	5.5	9	1.63
SEP2	4.5	7.5	1.66
SEP3	4.5	7.5	1.66
SEP4	4	7	1.75

The columns sizing was conducted according to [19] and refined using Aspen Plus V10 (RadFrac option).

P1S2 stripping column: From the calculation the diameter is 1.93 m. The overall efficiency is 0.7 and so, being 12 the number of sieve trays (13 with the reboiler), the total tower height is 10.44 m and a section head loss (hot liquid height) of 3.22 m.

STRIPPER stripping column: The column has 10 sieve trays, with kettle reboiler and a partial condenser. The overall efficiency is 0.5 so, the vertical height of the active tray section is 9.7 m with a diameter of 1.93 m and a section head loss of 0.816 m.

CRIO1 cryogenic column: The column has 13 sieve trays with a partial condenser, only. The overall efficiency is 0.7, the diameter 1.93 m, the section height 10.44 m and the section head loss 1.438 m.

ABSORBER absorption column: For packed columns, the only difference is the Height Equivalent to Theoretical Plate (HETP). The absorption column has 10 stages with no reboiler and condenser. The overall efficiency is 0.5 so the HETP is 1.217 m and the vertical height of the packed section is 15.8 m, with a diameter of 1.93 m.

The exchanger units (HeatX) are different for the *non-integrated* and the *retrofitted* process.

The heat transfer coefficient has not been considered as constant, but the specific values are reported in Table S27 (Supporting Information). The details on the utilities and exchanger sizing are reported in Tables S28-S30 for the Non-integrated plant and in Tables S31-S33 for the Retrofitted one.

The Pressure Swing Adsorption (PSA, Sep2) was specified with water split fraction of 1 in the water outlet stream and an ethylene split fraction of 0.33. All the other split fractions are equal to zero. The

steps of the PSA cycle are four: adsorption during pressurization, depressurization and, between these two main steps, the blowdown of one bed and the contemporaneous re-pressurisation of the other one.

The adsorption system was sized as a cylindrical pressure vessel containing the adsorbent. The head space is usually left empty and up to 20% of the volume between the tangent lines of the vessel is packed with inert material to ensure a uniform flow profile.

The amount of adsorbent required is calculated according to the following mass balance [26]

$$(F_1 y_1 - F_2 y_2) M_w t_a = 1000(m_1 - m_2) M_a f_L$$

where F_1 is the feed and F_2 the product molar flow rate (mol/s), y_1 is the feed and y_2 the product mole fraction of adsorbed component, M_w the molecular weight of adsorbed component (g/mol), t_a the duration of the adsorption stage of the cycle (s), m_1 and m_2 the maximum and minimum adsorbent loading (wt/wt adsorbent), M_a the mass of adsorbent bed (kg) and f_L the fraction of bed that is fully loaded at end of the adsorption phase.

The selected adsorbent is zeolite 13X. The fraction of the adsorbent bed, f_L , that reaches a loading m_1 at the end of the adsorption step of the cycle depends on the number of beds used. For a simple two-bed system it is typically less than 0.7. The total cycle time is equal to the time spent in adsorption multiplied by the number of beds in the sequence. A cycle time in the range 5 - 60 minutes can be assumed. The volume of each adsorbent bed is calculated from the mass of adsorbent and its bulk density. The details of PSA sizing are reported in Table S34 and S35 (Supporting Information). Total cycle duration was considered 6 min (3 min for each bed) [27].

6 EQUIPMENT COSTING

All the equipment costs were actualized to January 2019:

$$Cp_s = Cp_r \left(\frac{I_s}{I_r} \right)$$

where C_{p_s} , C_{p_r} are the prices of the equipment in year s or r , respectively, and I_s/I_r is the escalation ratio (ratio between the inflation indexes of years s and r). In this work, the *Chemical Engineering Plant Cost Index* (CEPCI) was used, as calculated in Table 5 [28]:

Table 5 CEPCI Index for cost escalation [28]

CEPCI JAN 2004	CEPCI JAN 2016	CEPCI JAN 2017	CEPCI JAN 2018	CEPCI JAN 2019
400	536.5	538.16	540.42	544.42

Reactors

The cost of the reactors has been evaluated in 2016 and actualized in 2019 as above described. The items were mapped as packed towers applied for absorption with SS316 as shell material and design temperature 380°C, design gauge pressure 243.6 kPa. The cost of the catalyst is set as 9.53 \$/kg reported at 2019 [19].

Flash drum separators

The items were mapped as vertical process vessels in SS316 steel. The fluid volume was the standard 20% and the design temperature is 125°C.

Distillation, absorption and stripping columns

The towers have uniform diameter with SS316 steel as shell material. The MDEA price has been assessed using the Sigma Aldrich website, since the amount of amine needed is 14.2 litres, only, for a price of 107.25 \$/L.

Heat Exchangers

The heat exchangers costs are reported in Tables from S36 to S39 (Supplementary Information) for both plant layouts and they were differently specified according to their type.

PSA

To evaluate the costs of the PSA [19] at least two adsorbent vessels were included, with the set of switching valves and any other equipment (blowers, vacuum pumps, or heaters) required for the regeneration of the material. Thus, an additional 10% has been added to the cost of the two adsorbent vessels calculated through the reference algorithms.

Pumps, mixers and compressors

Centrifugal single or multi-stage pumps and static mixers were chosen. The compressors were specified as centrifugal horizontal compressors, requiring the capacity, the inlet and outlet design gauge pressures, as reported in Table S40 (Supporting Information).

Full plant economics

After the evaluation of the cost of the single items, the cost of the entire plant was assessed, starting from the calculation of the Total Cost (TC), as the sum of the CAPital Expenditures (CAPEX) and the OPERating ones (OPEX) [19]. Additional profitability indexes were calculated from the TC, *e.g.* the net annual profit and the cash flow analysis. At last, the two most important parameters to confirm the feasibility of the process were obtained, *i.e.* the Net Present Value (NPV) and the Net Rate of Return (NRR) that, for a normal chemical plant should be about (and not less than) 10%.

The CAPEX are the sum of the fixed capital and the working capital.

The operating expenses (A_{TE}) are the sum of the Manufacturing Expenses (A_{ME}) and the General Expenses (A_{GE}). The A_{ME} are in turn divided into Direct Manufacturing (A_{DME}) and Indirect Manufacturing (A_{IME}) Expenses, while the A_{GE} are the sum of the General and Administrative (G&A), the Distribution and Selling (D&S) and the Research and Development (R&D) costs. The depreciation is generally considered apart due to its effect in the cash flow analysis. All the operating

expenses have been considered for a period of 20 years of production and with the 96% of operating hours a year (8406 h/y) and the plant has been set in the US.

CAPEX

The fixed capital (Table 6 and 7) was obtained from the sum of the contingency, the installation cost of the plant equipment inside and outside the “battery limits” (ISBL and OSBL). The ISBL cost have been assessed using the factorial method presented in [26] and the contingency was set as 21% of ISBL. The cost of the catalyst, as well as the cost of the MDEA, have been evaluated as operating costs since the reactor is considered to have a fixed bed configuration and the catalyst is considered to be changed once every six months, so twice a year, as well as the amine make-up. The working capital was estimated as the 15% of the fixed capital investment.

Table 6 Capital Expenses - non-integrated process

ISBL	109,674,254.83
OSBL	43,869,701.93
Contingency	23,031,593.52
Fixed capital, C_{FC}	176,575,550.28
Working Capital (15% of fixed capital), C_{WC}	26,486,332.54
Total capital investment, C_{TC} ($C_{FC}+C_{WC}$)	203,061,882.83

Table 7 Capital Expenses - retrofitted process

ISBL	105,983,274.28
OSBL	42,393,309.71
Contingency	22,256,487.60
Fixed capital, C_{FC}	170,633,071.59
Working Capital (15% of fixed capital), C_{WC}	25,594,960.74
Total capital investment, C_{TC} ($C_{FC}+C_{WC}$)	196,228,032.33

It should be noted that contrary to most cases, the retrofit decreased the number of heat exchangers, with lower installation costs.

OPEX

We obtained the prices of process steam, refrigerants, cooling water, etc. using the equations reported in [19]. Most of the US electricity is generated from coal and natural gas and is here assumed as purchased outside, with cost actualized to 2019 from [29].

The price of bioethanol (40 vol%) is a major item and has been decreased with respect to market cost by 50% due to savings in the purification by flash or feed split with respect to the azeotropic distillation [17,30]. Then it was actualized to 2019 [29] reaching a production cost of 0.293 \$/kg.

Other direct costs are: i) operating labour corresponding to 50,000 \$/y per 3 shift positions (almost all plants are operated on a shift-work basis with typically 4.8 operators per shift); ii) supervision and clerical labour, calculated as 15% of operating labour; iii) maintenance and repairs, considered as 5% of fixed capital investment; iv) operating supplies, 15% of maintenance and repairs; v) laboratory charges, 15% of operating labour; vi) patents and royalties, 3% of total expenses.

Indirect Manufacturing Expenses are social security, unemployment insurance and other compensation paid indirectly to plant personnel, which amount to *ca.* 60% of the direct salaries. These costs are the sum of the operating labour, supervision and maintenance. Other indirect expenses are local property taxes and insurance. These are assessed on the capital cost of the plant and, typically, a 3% of the fixed capital for both is taken. Tables 8 and 9 summarise the list of total direct and indirect costs.

As a comparison, in <http://joshuamayourian.com/static/ethylene.pdf> a detailed economic analysis of an ethylene production plant from cracking is reported. The process is different, implying higher utility consumption in the furnace and a wider product distribution, which implies much heavier cryogenic distillation. Despite this, the utilities cost is in the same order of magnitude of our work: 3.7 M\$/year for compression, 1.3 M\$/year for refrigeration and 10.4 M\$/year for the fractionation. The molar flow rate was in the same order of magnitude of our case, *ca.* 1000 kmol/h. Furthermore, in https://repository.upenn.edu/cgi/viewcontent.cgi?article=1036&context=cbe_sdr a calculation of installation and operation costs for the ethanol to ethylene process is reported. The utilities cost

amounted to 13.8 M\$, corresponding to 0.0062 \$/lb=13 \$/ton of ethylene and the order of magnitude is thus the same of the present case.

Table 8 Total Direct and Indirect Manufacturing Expenses - non-integrated process

Manufacturing expenses			Annual cost (\$/y)
Direct			
Raw materials			
	<i>kg/h</i>	<i>\$/kg</i>	
Bioethanol 40% vol	114,569.4	0.293	282,179,661.42
	<i>m³/h</i>	<i>\$/m³</i>	
Water	69.12	0.0869	50,498.52
	<i>\$/kg</i>	<i>kg/year</i>	
Catalyst	9.53	760.00	7,240.75
	<i>\$/l</i>	<i>l/year</i>	
MDEA	107.25	0.71	76.15
Operating labour (3 shift positions)			3,000,000.00
Supervisory and clerical labour (15% of operating labour)			450,000.00
Utilities			
	<i>kg/s</i>	<i>\$/kg</i>	
Steam	256.10	0.023	509,588.87
	<i>kWh</i>	<i>\$/kWh</i>	
Electricity	5,364.17	0.0786	3,544,169.15
	<i>kJ/h</i>	<i>\$/kJ</i>	
Refrigerant	54,279,791.63	0.000121	158,196.60
	<i>m³/h</i>	<i>\$/m³</i>	
Cooling water	1,298.89	0.07	2,229.38
Maintenance and repairs (5% of fixed capital)			8,828,777.51
Operating supplies (15% of maintenance & repairs)			1,324,316.62
Laboratory charges (15% of operating labour)			450,000.00
Patents & royalties (3% of total expense)			6,091,856.48
Total, ADME			306,596,611.50
Indirect			
Overhead (payroll and plant), packaging, storage (60% of operating labour, supervision, and maintenance)			7,367,266.51
Local taxes (2% of fixed capital)			3,531,511.01
Insurance (1% of fixed capital)			1,765,755.50
Total, AIME			12,664,533.02
Total Manufacturing expenses, AME=ADME+AIME			319,261,144.52

General expenses	
General & Administrative costs (8% of overhead)	589,381.32
Distribution and selling (10% of total expenses)	31,926,114.45
R&D (5% of total expenses)	15,963,057.23
Total general expense, A_{GE}	48,478,553.00
Salvage value, S (20% of the initial capital cost)	35,315,110.06
Depreciation (10% of fixed capital, or $(C_{FC}-S)/\text{years}$), A _{BD}	7,063,022.01

Table 9 Total Direct and Indirect Manufacturing Expenses - retrofitted process

Manufacturing expenses			Annual cost (\$/y)
Direct			
<i>Raw materials</i>			
	<i>kg/h</i>	<i>\$/kg</i>	
Bioethanol 40% vol	114,569.4	0.293	282,179,661.42
	<i>m³/h</i>	<i>\$/m³</i>	
Water	69.12	0.0869	50,498.53
	<i>\$/kg</i>	<i>kg/year</i>	
Catalyst	9.53	760.00	7,240.79
	<i>\$/l</i>	<i>l/year</i>	
MDEA	107.25	0.71	76.15
Operating labour (3 shift positions)			3,000,000.00
Supervisory and clerical labour (15% of operating labour)			450,000.00
<i>Utilities</i>			
	<i>kg/s</i>	<i>\$/kg</i>	
Steam	285.28	0.023	566,939.15
	<i>kWh</i>	<i>\$/kWh</i>	
Electricity	4,819.56	0.0786	3,184,342.15
	<i>kJ/h</i>	<i>\$/kJ</i>	
Refrigerant	54,279,791.63	0.000121	158,196.60
	<i>m³/h</i>	<i>\$/m³</i>	
Cooling water	2,609.11	0.07	4,478.22
Maintenance and repairs (5% of fixed capital)			8,531,653.58
Operating supplies (15% of maintenance & repairs)			1,279,748.04
Laboratory charges (15% of operating labour)			450,000.00
Patents & royalties (3% of total expense)			5,886,840.97
Total, ADME			305,749,675.58
Indirect			
Overhead (payroll and plant), packaging, storage (60% of operating labour, supervision, and maintenance)			7,188,992.15
Local taxes (2% of fixed capital)			3,412,661.43
Insurance (1% of fixed capital)			1,706,330.72
Total, AIME			12,307,984.30
Total Manufacturing expenses, AME=ADME+AIME			318,057,659.88

General expenses	
General & Administrative costs (8% of overhead)	575,119.37
Distribution and selling (10% of total expenses)	31,805,765.99
R&D (5% of total expenses)	15,902,882.99
Total general expense, A_{GE}	48,283,768.35
Salvage value, S (20% of the initial capital cost)	34,126,614.32
Depreciation (10% of fixed capital, or $(C_{FC}-S)/\text{years}$), A_{BD}	6,825,322.86

Total expenses and net annual profit

The total expenses, A_{TE} , are given by the sum of the total manufacturing expenses, A_{ME} , the general expenses, A_{GE} , and the depreciation, A_{BD} . The revenue from sales is obtained by the product between the annual capacity of the plant and the price at which ethylene, the product, is sold. In this work, being the price of ethylene a market variable, it has been chosen the minimum price at which the process is profitable, *i.e.* $NRR > 10\%$. The net annual profit, A_{NP} , was calculated as the difference between the revenues from sales and the total expenses and, accordingly, the net annual profit after taxes, A_{NNP} , subtracting the income taxes, A_{IT} , calculated as 35% of the net annual profit. The results for both the non-integrated and the retrofitted process are reported in Table 10.

Table 10 Net Annual Profit After Taxes

	Non-integrated process		
	Plant Capacity (kg/y)	Selling price of ethylene (\$/kg)	Annual cost (\$/y)
Revenue from sales, A_s	445,652,343.95	1.165	519,184,980.70
Net annual profit ($A_s - A_{TE}$), A_{NP}			144,382,261.17
Income taxes, A_{IT} (35% of A_{NP})			50,533,791.41
Net annual profit after taxes ($A_{NP} - A_{IT}$), A_{NNP}			93,848,469.76
	Retrofitted		
Revenue from sales, A_s	445,652,343.95	1.152	513,391,500.23
Net annual profit ($A_s - A_{TE}$), A_{NP}			140,224,749.13
Income taxes, A_{IT} (35% of A_{NP})			49,078,662.20
Net annual profit after taxes ($A_{NP} - A_{IT}$), A_{NNP}			91,146,086.94

The cash flow has been evaluated assuming that the period of construction of the plant is 3 years [26]. To normalize dollars to the same point in time, annual cash flows are multiplied by discount factors, a decimal number calculated as:

$$discount\ factor\ (df) = \frac{1}{(1+r)^T}$$

where, r is the discount rate and T is the year. The discount rate refers to the interest rate used to determine the present value. The discount factor calculated is multiplied by a cash flow value to discount it back to the present value.

$$annual\ discounted\ (\$) = df * A_{NCI}$$

where A_{NCI} is the Net Cash Income found in the cash flow analysis. If the net present value is positive, the project is economically viable, otherwise financially unfeasible. Cumulative cash flow data at different discount rates are reported in Figures 7 and 8 for the non-integrated and the retrofitted processes, respectively. The net present value, NPV, is the final cumulative discounted cash flow value at project conclusion.

Figure 7 Cumulative discounted cash flow at 0%, 10% or 15% discount rates

- non-integrated process

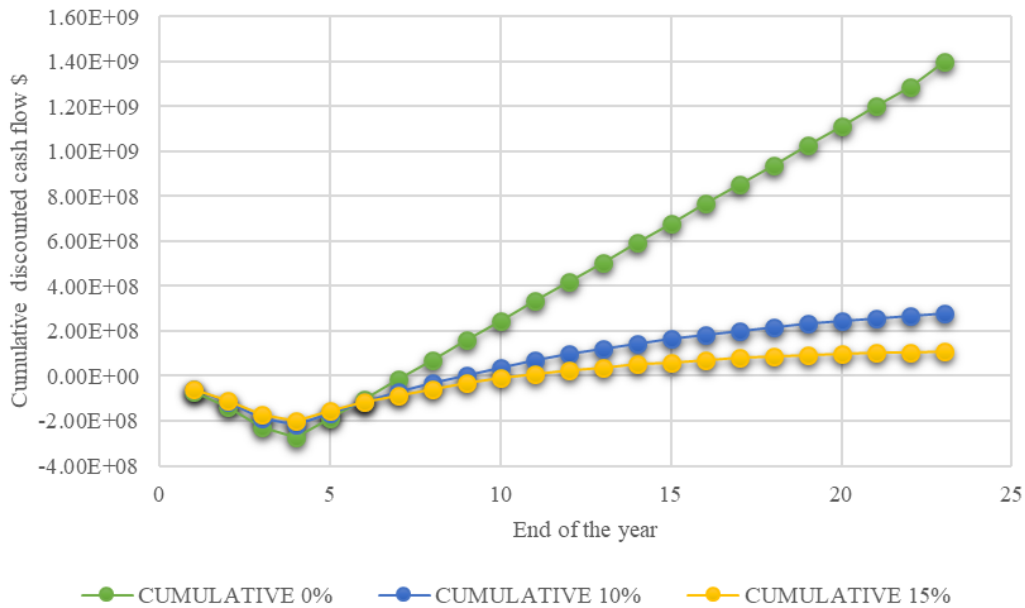
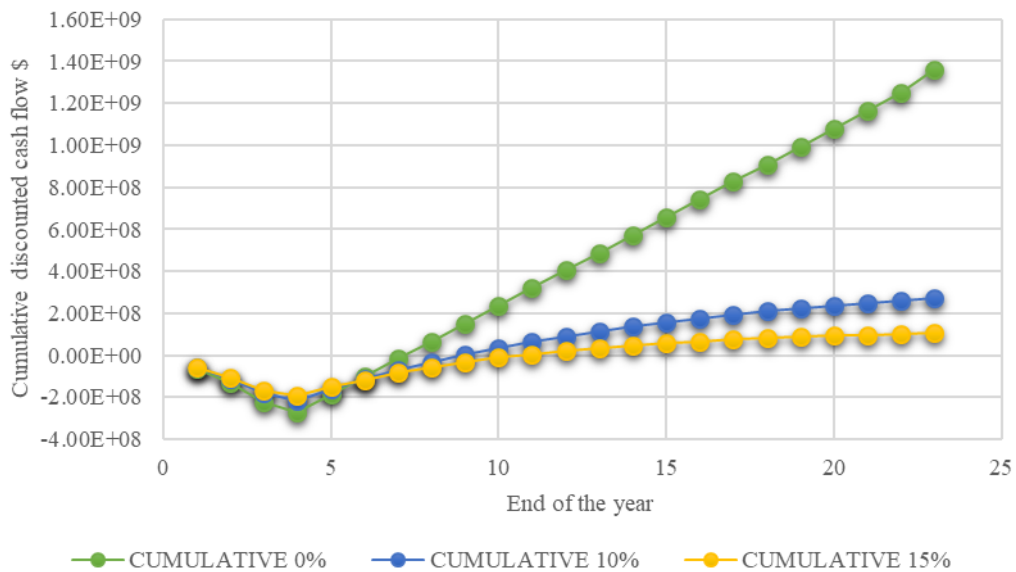


Figure 8 Cumulative discounted cash flow at 0%, 10% or 15% discount rates - retrofitted process



To evaluate the NPV, a discount rate $\geq 10\%$ was considered reliable. The payback-period (PBP) is the time that must elapse following the start-up before the cumulative undiscounted cash flow repays the fixed capital investment. The payback period, *i.e.* the point where undiscounted cash flow overcomes the level of negative working capital, was 10 years for the non-integrated and 9 years for the retrofitted processes. The discounted break-even point (DBEP, the time until the discounted

cumulative cash flow becomes positive) was also 9 years for both plants. The NPV is directly connected with the ethylene selling price, that has been chosen to have the same profitability (NRR) in the two processes.

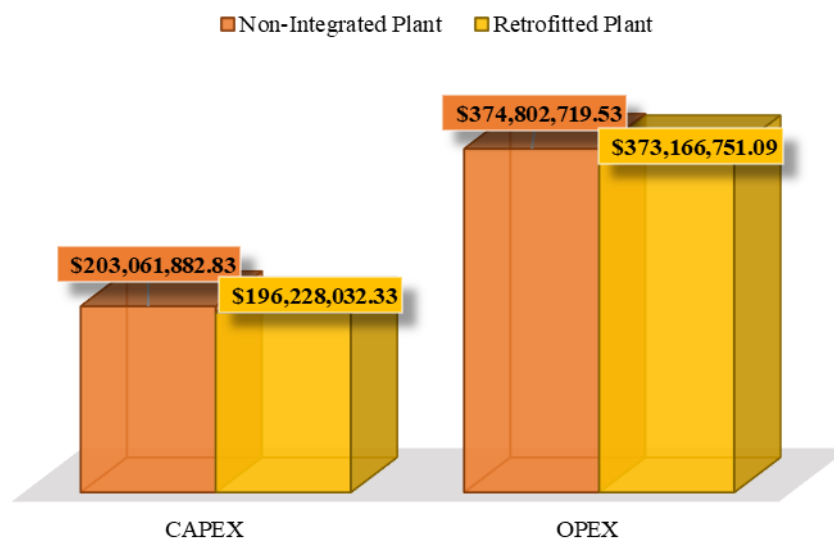
The net rate of return value, NRR, or the best measure of project profitability, has been assessed as:

$$NRR = \frac{(1,5 \times NPV)}{n' \times C_{TC}(i=\text{cost of capital})} \times 100$$

Where n' is the operating lifetime (20 years) plus one-half the time proceeding the start-up (n' = 21.5 years). The NRR value results 10.3% for both plants, being the C_{TC} 1.88 10⁸ and 1.82 10⁸ \$ for the non-integrated and the retrofitted processes, respectively.

As a summary, Fig. 9 compares CAPEX and OPEX for both process options.

Figure 9 Total CAPEX and OPEX comparison



Being the retrofitted process the most profitable one, it will be considered in the following as best option.

The cost of ethylene production mainly depends on the ethanol production cost. Indeed, by increasing the latter from 0.293 to 0.65 and 1 \$/kg, the ethylene selling price increased linearly from 1.15 to 2.102 and 3.034 \$/kg, respectively, by keeping NRR fixed at 10.3%. The effect on NRR and NPV of the variation of other parameters is reported in the sensitivity analyses (Figures 10 and 11). The starting point of the sensitivity plots (0%) corresponds to the base case for the retrofitted process

reported in this work: tax rate of 35%, diluted ethanol cost of 0.293\$/kg, ethylene selling price of 1.152 \$/kg, NPV of 181,893,230.46 \$ and a total capital investment of 196,228,032.33\$, for a NRR of 10.3%.

Figure 10 Sensitivity analysis NRR (%) vs. Cost Variation (%).

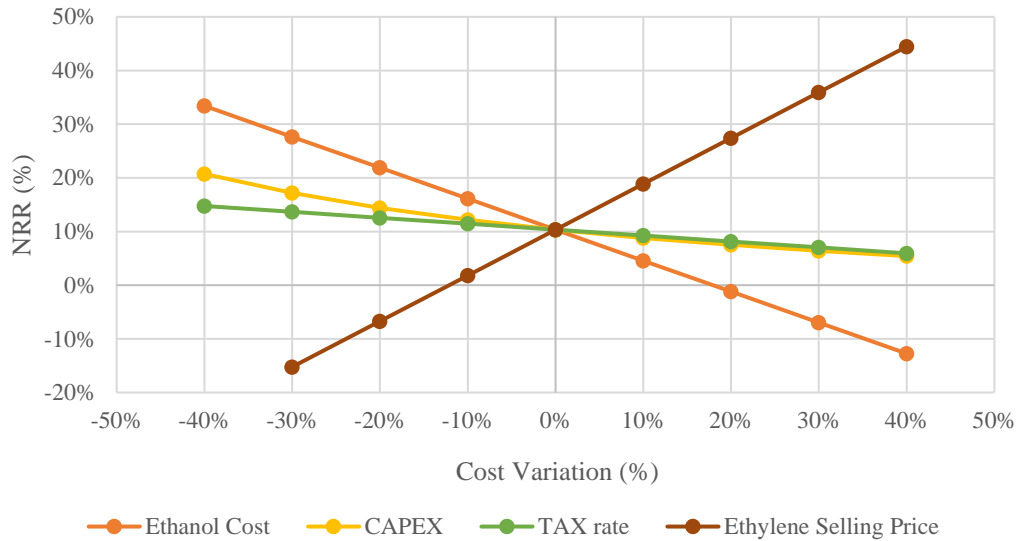
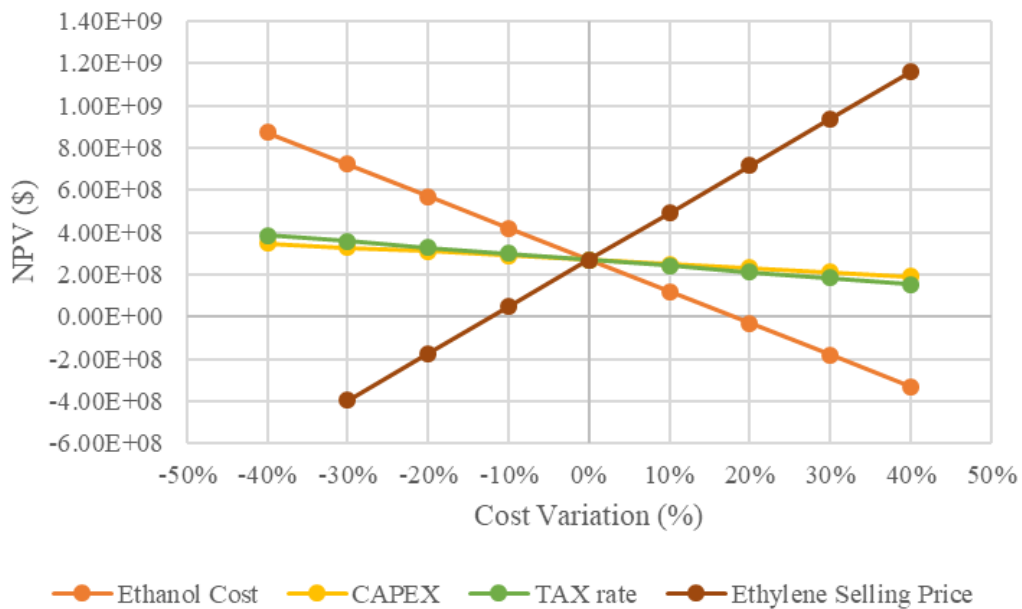


Figure 11 Sensitivity analysis NPV (\$) vs. Cost Variation (%).



The most important conclusion of this work is that both the non-integrated plant and the retrofitted one can be very competitive in the worldwide bioethanol-to-bioethylene route, even with Brazil and

India, provided that the diluted (40 vol%) ethanol cost is 0.293 \$/kg (Fig. 12). Indeed, Fig. 12 reports the ethylene production costs from bio-ethanol in different countries, based on the local ethanol cost. Brazil bioethanol is intended from sugar cane, US from corn, EU from sugar beets and China from diversified supplies, such as sweet sorghum [31]. Moreover, if the ethylene produced with the retrofitted process is sold at the same price achieved with the non-integrated process (higher), the net rate of return of the process would increase up to 11.3%, thus confirming the best profitability among the two options.

Furthermore, the cost of ethylene production mainly depends on the ethanol price. The original purchase cost of bioethanol was assumed to be halved due to lower purification costs when using diluted bioethanol [29,30]. However, the enhancement of the cost of ethanol from 0.293 to 0.65 \$/kg, the final production cost of ethylene becomes 2,102 \$/ton, which is still competitive for settling the plant in US and Europe. From the sensitivity analyses, it is clear that the best range of ethanol cost to make competitive the process ranges between 0.293 and 0.65 \$/kg. The analysis does not take into account the raw materials cost (e.g. sugar price or production/purification route) to produce diluted bioethanol, it only considers its entry price. Furthermore, when increasing by 10 % the ethylene selling price, the process will have a NRR of 20-26%; hence, doubling its profitability.

Of course, all these bio-ethylene process are still 1.5-2 times higher than petrochemical one in most cases, but considering that ethylene conventional production routes lead to a production cost variable between 600 and 1,300 \$/ton, the key feature to use less expensive feedstocks for bioethanol such as the here proposed diluted bioethanol streams, is the key to improve the economic viability of the process..

Figure 12 Production cost per ton of bio-ethylene in different countries in the world compared with the new plants studied [31].



7 CONCLUSIONS

The very first layout of a bioethanol-to-bioethylene plant is here reported, allowing double ethylene capacity with respect to the current biggest facility for this process. As a main novelty it exploits diluted bioethanol as a less expensive raw material. The plant design has been accomplished with full sizing of every item and thermal management optimisation. A further improvement in sustainability is achieved by substituting the caustic wash (and thus waste) during the CO₂ recovery step with a reversible and cyclic MDEA absorption step. The thermally integrated plant (retrofitted) is characterised by lower utilities consumption, but also by a lower number of heat exchangers. Consequently, it is the less expensive and most remunerative from every point of view.

The economic feasibility of the process has been assessed for a 20 years project. The most important achievement is that both plant layouts can be economically feasible and competitive in the worldwide ethylene production from ethanol, provided that sufficiently low-cost diluted ethanol is available (0.293 \$/kg for a 40 vol% solution). It can be still competitive with US and European facilities when

considering an ethanol cost up to 0.65 \$/kg. Double profitability can be achieved when increasing the ethylene selling price by 10%, only.

It should be specified that no selling of by-products has been considered and no CO₂ selling options has been included in this study that would add revenues, but also increase installation and operation costs.

REFERENCES

- [1] A. Morschbacker, *Polym. Rev.* 49(2) (2009) 79–84. 10.1080/15583720902834791.
- [2] J. Sun., Y. Wang, *ACS Catal.* 4 (2014) 1078–90. dx.doi.org/10.1021/cs4011343.
- [3] Ethylene from Ethanol, Chematur Engineering AB. Available at:
<https://chematur.se/technologies/bio-chemicals/bio-ethylene-ethene/>.
- [4] “I’m Green Polyethylene.” [Online]. Available:
<http://plasticoverde.braskem.com.br/site.aspx/Im-greenTM-Polyethylene>. [Accessed: 23-Apr-2019].
- [5]
www.technip.com/sites/default/files/technip/publications/attachments/Ethylene_production.pdf.
- [6] “The Ethylene Technology Report 2016 - Research and Markets”.
www.researchandmarkets.com.
- [7] I.S. Yakovleva., S.P. Banzaraksheva., E. V. Ovchinnikova., V.A. Chumachenko., L.A. Isupova, *Katal. v Promyshlennosti* 16(1) (2016) 57–73. 10.18412/1816-0387-2016-1-57-73.
- [8] D. Fan., D.J. Dai., H.S. Wu, *Materials (Basel)*. 6(1) (2013) 101–15. 10.3390/ma6010101.
- [9] J. Althoff., K. Biesheuvel., A. De Kok., H. Pelt., M. Ruitenbeek., G. Spork., J. Tange., R. Wevers, *ChemSusChem* 6(9) (2013) 1625–30. 10.1002/cssc.201300478.
- [10] M. Arvidsson., L. BJORN, Process integration study of a biorefinery producing ethylene from lignocellulosic feedstock for a chemical cluster, available at

<http://publications.lib.chalmers.se/records/fulltext/140886.pdf>. Chalmers University of Technology, Goteborg (SE), 2011.

- [11] I.D. Posen,, W.M. Griffin,, H.S. Matthews,, I.L. Azevedo, *Environ. Sci. Technol.* 49(1) (2015) 93–102. 10.1021/es503521r.
- [12] J.M.R. Gallo,, J.M.C. Bueno,, U. Schuchardt, *J. Braz. Chem. Soc.* 25(12) (2014) 2229–43. 10.5935/0103-5053.20140272.
- [13] P.A. Bastidas,, I.D. Gil,, G. Rodriguez, 20th Eurpean Symp. Comput. Aided Process Eng. - ESCAPE20 (2010) 1–6.
- [14] I. Rossetti,, A. Tripodi,, E. Bahadori,, G. Ramis, *Chem Eng Trans* 65 (2018) 73–8. 10.3303/CET1865013.
- [15] G. Ramis,, I. Rossetti,, A. Tripodi,, M. Compagnoni, Diluted bioethanol solutions for the production of hydrogen and ethylene, Vol. 57, 2017.
- [16] I. Rossetti,, M. Compagnoni,, E. Finocchio,, G. Ramis,, A. Di Michele,, Y. Millot,, S. Dzwigaj, *Appl. Catal. B Environ.* 210 (2017) 407–20. 10.1016/j.apcatb.2017.04.007.
- [17] I. Rossetti,, M. Compagnoni,, G. De Guido,, L. Pellegrini,, G. Ramis,, S. Dzwigaj, *Canad. J. Chem. Eng.* 95 (2017) 1752.
- [18] A. Tripodi,, M. Belotti,, I. Rossetti, *ACS Sustain. Chem. Eng.* 7(15) (2019) 13333–50. 10.1021/acssuschemeng.9b02579.
- [19] Gael D.Ulrich, Palligarnai T. Vasudevan, *Chemical Engineering Process Design and Economics, A Practical Guide*, 2004.
- [20] G. Chen,, S. Li,, F. Jiao,, Q. Yuan, *Catal. Today* 125(1–2) (2007) 111–9. 10.1016/j.cattod.2007.01.071.
- [21] B. Rehm,, A. Haghshenas, *Underbalanced Drill. Limits Extrem.* (2012) 39–58. 10.1016/B978-1-933762-05-0.50009-7.
- [22] A. Tripodi,, M. Compagnoni,, E. Bahadori,, I. Rossetti,, G. Ramis, *Top. Catal.* 61(18–19) (2018) 1832. 10.1007/s11244-018-1002-6.

- [23] A. Erfani,, S. Boroojerdi,, A. Dehghani, *Pet. Coal* 57(1) (2015) 85–92.
- [24] F. Al Obaidi,, Z. Ye,, S. Zhu, *Macromol. Chem. Phys.* 204 (2003) 1653–9.
- [25] J. Becerra,, E. Quiroga,, E. Tello,, M. Figueredo,, M. Cobo, *J. Environ. Chem. Eng.* 6(5) (2018) 6165–74. 10.1016/j.jece.2018.09.035.
- [26] G. Towler,, R. Sinnott, *Chemical Engineering Design. Principles, Practice and Economics of Plant and Process Design*, Vol. 53, 2013.
- [27] K.M. Kim,, H.T. Oh,, S.J. Lim,, K. Ho,, Y. Park,, C.H. Lee, *J. Chem. Eng. Data* 61(4) (2016) 1547–54. 10.1021/acs.jced.5b00927.
- [28] CEPCI values. Available at: <https://www.chemengonline.com/economic-indicators-cepci/>.
- [29] M. Compagnoni,, E. Mostafavi,, A. Tripodi,, N. Mahinpey,, I. Rossetti, *Energy&Fuels* 31(11) (2017) 12988–96.
- [30] I. Rossetti,, J. Lasso,, M. Compagnoni,, G. De Guido,, L. Pellegrini, *Chem. Eng. Trans.* 43 (2015) 229–34. 10.3303/CET1543039.
- [31] A. Mohsenzadeh,, A. Zamani,, M.J. Taherzadeh, *ChemBio Eng. Rev.* 4(2) (2017) 75–91. 10.1002/cben.201600025.